

Full Paper

On-Line Electrochemistry/Electrospray Ionization Mass Spectrometry (EC/ESI-MS) for the Generation and Identification of Nucleotide Oxidation Products

Anne Baumann, Wiebke Lohmann, Sandra Jahn, Uwe Karst*

University of Münster, Institute of Inorganic and Analytical Chemistry, Corrensstr. 30, 48149 Münster, Germany

*e-mail: uk@uni-muenster.de

Received: July 14, 2009

Accepted: September 26, 2009

Abstract

The oxidation behavior of DNA and RNA nucleotides is studied by an on-line set-up consisting of an electrochemical thin-layer cell (EC) directly coupled to electrospray ionization mass spectrometry (ESI-MS). This set-up allows the generation of nucleotide oxidation products in the electrochemical cell at increasing potentials. Moreover, the products are determined directly, without isolation or derivatization steps, by electrospray ionization time of flight mass spectrometry (ESI-ToF/MS). The dependence of the mass spectra on the applied potential is displayed as 'mass voltammograms'. An advanced set-up, consisting of the electrochemical cell coupled to electrospray ionization tandem mass spectrometry (EC/ESI-MS/MS) allows further structure elucidation based on fragmentation experiments. The electrochemical conversion is performed using a boron doped diamond (BDD) working electrode, which is known to generate hydroxyl radicals at high potentials. The capability of the EC-MS system to generate highly relevant oxidation products which also occur upon oxidative damage in vivo is demonstrated in this study by the formation of well known biomarkers for DNA damage, including 2'-deoxy-8-oxo-guanosine 5'-monophosphate.

Keywords: DNA damage, Electrochemistry, Mass spectrometry, Nucleotides, 8-Oxo-guanosine

DOI: 10.1002/elan.200900358

1. Introduction

Modification of nucleotides along DNA strands are intensively studied processes, as these damages and mutations play a crucial role in mutagenesis, carcinogenesis and aging. In recent years, oxidative DNA damage caused by reactive oxygen species (ROS) like hydrogen peroxide, hydroxyl radicals, nitric oxide, and superoxide has become of major interest in this research area [1–4]. ROS are endogenous species, arising from various cellular processes in the organism. Macrophages are known to produce numerous radicals, including superoxide and nitric oxide. Hydrogen peroxide, arising from peroxisomes as well as during the reduction of oxygen can undergo subsequent reaction with catalytically acting traces of metal ions to hydroxyl radicals. Hydroxyl radicals are highly reactive and can attack DNA by abstracting hydrogen atoms or by direct adduct formation with nucleobases. Depending on the type of modification, the oxidized nucleobases can be removed by enzymatic repair mechanisms, but they can also cause depurination, base mispairing and strand scissions, with the final consequence being apoptosis or cancer promotion [2, 5, 6].

Electrochemical techniques have been applied in the analysis of DNA oxidation processes with different objectives. After the discovery of oxidized nucleotides, nucleosides and nucleobases as important biomarkers in cell extract and body fluids, high performance liquid chroma-

tography with electrochemical detection has been implemented as efficient analytical method in the determination of these biomarkers [7, 8]. Moreover, cyclic voltammetry (CV) has been used in numerous studies in order to estimate oxidation potentials and oxidation mechanisms of nucleotides, nucleosides and bases [9–12]. A comparison of the oxidation peaks of different nucleotides by differential pulse voltammetry shows that guanosine 5'-monophosphate (GMP) requires the lowest oxidation potential of all four nucleotides [9]. The products generated upon oxidation have been studied by spectrometric techniques [11]. Additionally, stable oxidation products have been isolated and further characterized by nuclear magnetic resonance (NMR) as well as by gas chromatography (GC) after derivatization into volatile products [10]. Besides bare electrode surfaces, modified glassy carbon electrodes have been implemented for studying DNA oxidation processes. [13, 14]. Electrochemical DNA sensors, generally consisting of single stranded DNA, immobilized on glassy carbon electrode surfaces, can bind highly specific to target DNA strands [15]. The analysis of not only nucleotides but entire DNA strands by electrochemical techniques has become of particular interest, revealing that both, holes and electrons can migrate through the DNA helix over distances [12, 16]. Friedmann and Heller reported the distribution of guanosine (G) along the DNA as a natural way to protect exons, protein coding DNA sequences, from oxidative damage

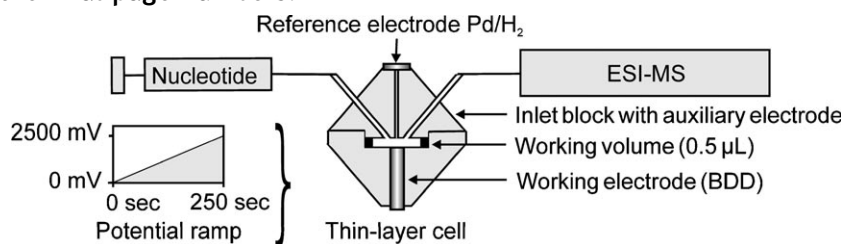


Fig. 1. Experimental set-up for the simulation of oxidation processes of nucleotides. For generation of mass voltammograms, the electrochemical cell is coupled to ESI-ToF/MS and the potential is ramped between 0 and +2500 mV.

[17]. High average mole fractions of triplet G near the 5'-termini of introns, and very close to the 3'-termini of exons, can act as sinks for positive charge, thus preventing oxidative damage in protein coding DNA regions.

Aiming the electrochemical analysis of nucleotides in combination with direct product identification, requiring no product isolation or derivatization steps, electrochemistry coupled on-line to electrospray ionization mass spectrometry (EC/ESI-MS) is a promising tool. The on-line EC/ESI-MS set-up has been introduced about 20 years ago and has since been used to study redox reactions of various biomolecules [18–22]. Getek et al. coupled a coulometric flow-through cell with a glassy carbon working electrode to a thermospray MS and studied the oxidation behavior of acetaminophen [23]. Deng and van Berkel used a homemade thin-layer cell, on-line connected to ESI-MS and analyzed the dopamine redox system [24]. Based on these early studies, it soon became apparent that this newly developed technique offers interesting features for the simulation of oxidative drug metabolism (phase I metabolism) [25–29]. In contrast to existing in vivo and in vitro methods, this purely instrumental technique enables the direct detection of reactive intermediates, which in the organism may undergo subsequent reactions with endogenous compounds [27]. Bruins and co-workers systematically investigated the oxidation reactions being simulated in a coulometric flow-through cell, equipped with a glassy carbon working electrode and determined aromatic hydroxylation, *N*-dealkylation, dehydrogenation, *N*-oxide and *S*-oxide formation as reactions being readily simulated by EC [28]. Furthermore, using a thin-layer cell with a platinum working electrode and oxidation potentials up to 2.0 V, the hydroxylation in aliphatic and allylic position has been demonstrated for the drug tetrazepam [29]. The group of Brajter-Toth recently studied the oxidation behavior of uric acid in an on-line EC-MS set-up. Uric acid is a product of the nucleotide catabolism in humans and is structurally closely related to 8-oxo-guanosine. The on-line set-up consisted of an electrochemical cell which is integrated in the spray needle of the electrospray interface [30]. Using this set-up, they determined dimeric uric acid oxidation products as well as degradation products including allantoin and alloxan monohydrate.

In the present study, the coupling of EC and ESI-MS is implemented as a tool to study nucleotide oxidation processes. The nucleotides are oxidized in an electrochem-

ical cell, which is coupled on-line either to electrospray ionization time of flight mass spectrometry (EC/ESI-ToF/MS) or electrospray ionization tandem mass spectrometry (EC/ESI-MS/MS) (Fig. 1). The electrochemical cell in this set-up is a thin-layer cell with exchangeable working electrode material. For the oxidation of nucleotides, the cell is equipped with a boron doped diamond (BDD) working electrode. BDD has a high overpotential for the generation of hydrogen and oxygen and therefore an enlarged potential window of up to 2500 mV in aqueous media. Another important feature is the efficient anodic generation of hydroxyl radicals on BDD surfaces at high potential [31–33]. As described above, hydroxyl radicals play an important role in oxidative DNA damage in vivo. Hence, an electrochemical system, in which the nucleotides are oxidized via direct electron abstraction as well as by reaction with hydroxyl radicals, including hydrogen abstraction as well as adduct formation, has the potential to mimic the oxidation processes occurring in vivo.

2. Experimental

2.1. Chemicals

The five nucleotides 2'-deoxyguanosine 5'-monophosphate (dGMP) sodium salt, 2'-deoxyadenosine 5'-monophosphate (dAMP) sodium salt, 2'-deoxycytidine 5'-monophosphate (dCMP) sodium salt, 2'-deoxythymidine 5'-monophosphate (dTMP) (free acid) and 2'-deoxyuridine 5'-monophosphate (dUMP) disodium salt were obtained from Sigma Aldrich (Steinheim, Germany). Ammonium acetate (NH₄Ac), and nitrous acid (65%) were obtained from Fluka Chemie (Buchs, Switzerland). Purified water for sample dilution was generated by a Milli-Q Gradient A 10 system and filtered through a 0.22 µm Millipak 40 filter unit (Millipore, Billerica, MA, USA). All Chemicals were used in the highest quality available.

2.2. Generation of Mass Voltammograms

Mass voltammograms were generated by coupling the electrochemical cell (ReactorCell, Antec Leyden, Zoeterwoude, The Netherlands) directly to the electrospray source of a time of flight mass spectrometer (micrOTOF, Bruker

Daltonics, Bremen, Germany) (Fig. 1). The cell was equipped with a BDD working electrode and the working volume amounts 0.5 μL . The potential was ramped between 0 and 2500 mV versus Pd/H₂ at a scan rate of 10 mV/s. Potentials were applied using either the electrochemical potentiostat ROXY (Antec Leyden) or a homemade potentiostat. The parameters of the mass spectrometer, operating in negative ion mode, were as follows: nebulizer (N₂): 0.8 bar; dry gas (N₂): 3.3 L/min; dry heater: 180 °C; capillary: 4 kV; endplate offset: 500 V; capillary exit: -129 V; skimmer 1: -43; skimmer 2: -25.5; hexapole 1: -25.5; hexapole 2: -22.1; hexapole RF: 90 V; lens transfer time: 49 μs ; pre puls storage time: 1.0 μs ; lens 1 storage: -30 V; lens 1 extraction: -20.9; lens 2: -12 V; lens 3: 16 V; lens 4: -3 V; lens 5: 30 V; mass to charge ratio (m/z) range: 100–800 m/z . The nucleotide solution with a concentration of 10 μM nucleotide was passed through the cell at a flow rate of 10 $\mu\text{L}/\text{min}$ by a syringe pump model 74900 (Cole Parmer, Vernon Hills, IL, USA). Each mass voltammogram was recorded at least three times to ensure reproducibility of the measurements.

2.3. Fragmentation Experiments

For fragmentation experiments, the electrochemical cell (ReactorCell) with a BDD electrode was coupled directly to a QTrap mass spectrometer (Applied Biosystems, Darmstadt, Germany), equipped with an electrospray ionization source. Instead of using the potential ramp shown in Figure 1, the potential of the cell was kept constant at 2500 mV for fragmentation experiments. A 100 μM nucleotide solution in water was passed through the cell at a flow rate of 10 $\mu\text{L}/\text{min}$ by a syringe pump. The optimized conditions used for the MS/MS experiments were as follows: negative ion mode; curtain gas (N₂): 1.03 bar (15 psi); ion spray voltage: -3500 V; temperature: 100 °C; nebulizer gas (N₂): 1.38 bar (20 psi); dry gas (N₂): 1.38 bar (20 psi); declustering potential: -15 V; entrance potential: -1 V; cell entrance potential: -17 V; collision energy: 50 V; collision energy spread: 15 V.

3. Results and Discussion

3.1. Mass Voltammograms

The oxidation behavior of the nucleotides dGMP, dAMP, dCMP, dTMP and dUMP was studied in an on-line set-up, consisting of an electrochemical cell, coupled directly to a time of flight mass spectrometer equipped with an electrospray ionization source. For each nucleotide, the measured data were converted into three dimensional plots, so called mass voltammograms, showing the ion intensity detected in the mass spectrometer as a function of the mass to charge ratio and the potential ramp applied in the electrochemical cell. The three dimensional plot provides a very good overview of all products generated upon oxidation and

These are not the final page numbers! ↗

enables the fast detection of unforeseen products. A section of the mass voltammogram of dGMP is shown in Figure 2.

For optimization of the EC/ESI-ToF/MS system, the extracted ion traces of dGMP and of the dGMP oxidation products, identified in the mass voltammograms (Fig. 2), were compared under varying conditions (Fig. 3). DGMP sodium salt, dissolved in pure water as well as in solutions with increasing concentrations of NH₄Ac (100 μM and 1000 μM) was tested for oxidation. In all three cases the oxidation of dGMP begins about 150 s (1500 mV) after starting the potential ramp, which becomes apparent by a signal decrease of dGMP and a signal increase for the oxidation products. The ion traces of the oxidation products in pure water and in 100 μM NH₄Ac solution show comparable intensities for both solutions. Increasing the NH₄Ac concentration up to 1000 μM results in significantly decreasing signal intensities for dGMP and for the mass traces m/z 362, 352, 293. It is likely that the decreasing intensities result from ion suppression effects in the electrospray interface. Hence, mass voltammograms of all five nucleotides were measured in water without additional electrolyte.

During further optimization steps, the oxidation of dGMP was carried out with and without previous activation of the BDD electrode, using 0.5 M nitric acid and a potential scan between -1500 and 1500 mV at a scan rate of 50 mV/s. No significant increase in the conversion rate of the nucleotides was observed after activation, even though variations in the intensities of the oxidation products were observed. The dGMP solution was also passed through the cell at different flow rates. Lowering the flow rate below 10 $\mu\text{L}/\text{min}$ resulted in an increase in the oxidative conversion of dGMP, but no

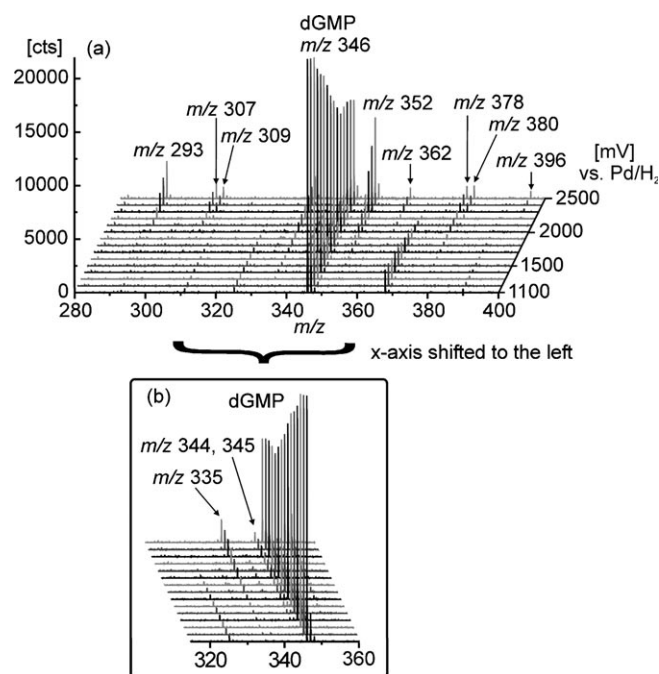


Fig. 2. Section of the mass voltammogram of dGMP, generated an on-line set-up consisting of EC/ESI-ToF/MS. (a) x-axis shifted to the right, (b) x-axis shifted to the left.

These are not the final page numbers!

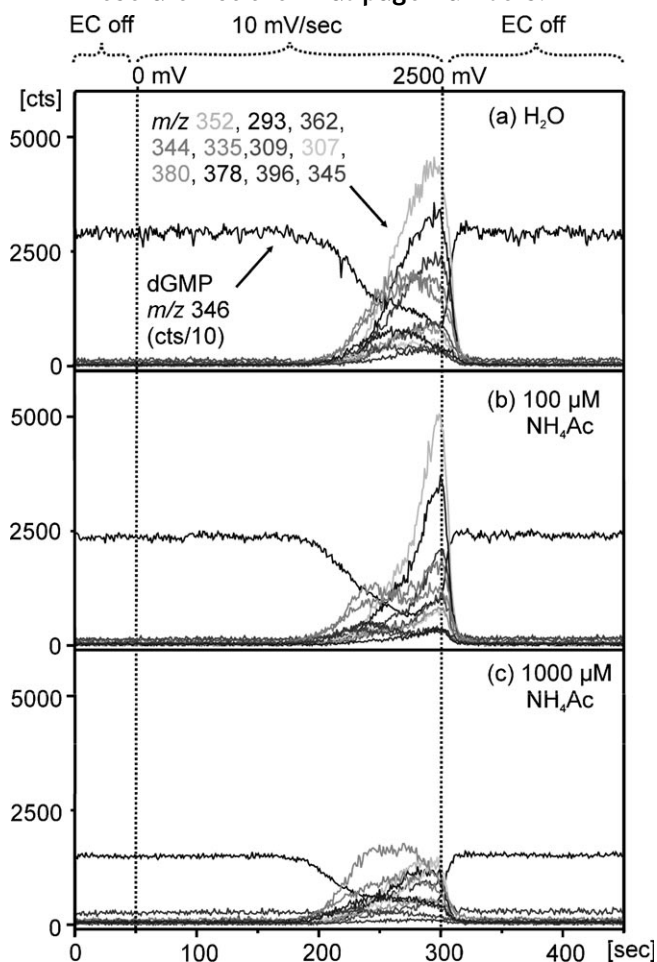


Fig. 3. Ion traces of dGMP and its oxidation products at increasing oxidation potentials (10 mV/s). DGMP sodium salt is dissolved in (a) pure water, (b) 100 μM and (c) 1000 μM NH_4Ac solution and oxidized in the EC/ESI-ToF/MS system.

signal increase of the oxidation products and no further oxidation products were observed.

3.2. Oxidation of Nucleotides by EC/ESI-MS

In the mass voltammogram of dGMP in Figure 2, the dGMP signal decreases at a potential of about 1500 mV. In parallel to the signal of dGMP, a second signal with a m/z of 368, correlating to a dGMP sodium adduct, decreases at increasing potential. Different products are generated upon oxidation, reaching their maximum signal intensity at the maximum potential of 2500 mV. The determination of the m/z values of the oxidation products enables the calculation of molecular formulas and thus of the modification of dGMP upon oxidation (Table 1).

To gain further structural information, the oxidation products were studied by EC/ESI-MS/MS. The fragmentation experiments were performed by applying a constant potential of 2500 mV in the electrochemical cell, which was directly coupled to a tandem mass spectrometer. Since the mass voltammogram already reveals maximum signal

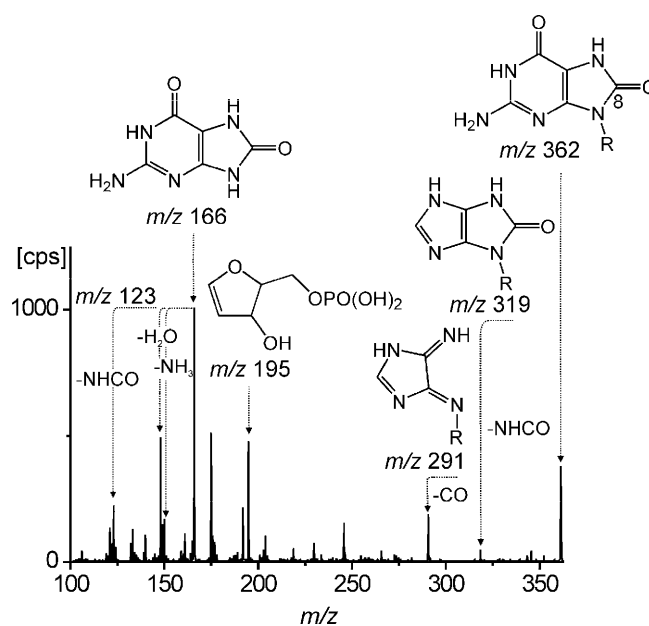


Fig. 4. Product ion spectra of the dGMP + O oxidation product obtained by EC/ESI-MS/MS. The fragmentation pattern is consistent with the formation of 8-oxo-dGMP upon oxidation.

Table 1. Molecular formulas of the dGMP oxidation products determined by EC/ESI-ToF/MS (deviation between the measured m/z and the calculated m/z < 5 ppm).

Measured m/z	Molecular formula	Transformation of dGMP
346.0546	$\text{C}_{10}\text{H}_{13}\text{N}_5\text{O}_7\text{P}_1$	–
293.0168	$\text{C}_8\text{H}_{10}\text{N}_2\text{O}_8\text{P}_1$	$-2\text{C}-3\text{H}-3\text{N} + \text{O}$
307.0440	$\text{C}_8\text{H}_{12}\text{N}_4\text{O}_7\text{P}_1$	$-2\text{C}-\text{H}-\text{N}$
309.0579	$\text{C}_8\text{H}_{14}\text{N}_4\text{O}_7\text{P}_1$	$-2\text{C}-\text{N} + \text{H}$
335.0406	$\text{C}_9\text{H}_{12}\text{N}_4\text{O}_8\text{P}_1$	$-\text{C}-\text{H}-\text{N} + \text{O}$
344.039	$\text{C}_{10}\text{H}_{11}\text{N}_5\text{O}_7\text{P}_1$	-2H
345.0469	$\text{C}_{10}\text{H}_{12}\text{N}_5\text{O}_7\text{P}_1$	$-\text{H}$
352.0640	$\text{C}_9\text{H}_{13}\text{N}_5\text{O}_8\text{P}_1$	$-\text{C} + \text{O} + 2\text{H}$
362.0498	$\text{C}_{10}\text{H}_{13}\text{N}_5\text{O}_8\text{P}_1$	$+\text{O}$
378.0445	$\text{C}_{10}\text{H}_{13}\text{N}_5\text{O}_9\text{P}_1$	$+2\text{O}$
380.0602	$\text{C}_{10}\text{H}_{15}\text{N}_5\text{O}_9\text{P}_1$	$+2\text{O} + 2\text{H}$
396.0564	$\text{C}_{10}\text{H}_{15}\text{N}_5\text{O}_{10}\text{P}_1$	$+3\text{O} + 2\text{H}$

intensity for all oxidation products at 2500 mV, this oxidation potential was chosen for fragmentation experiments. Using the EC/ESI-MS/MS set-up, the ions of the oxidation products can be subsequently extracted and product ion spectra of each oxidation product can be generated. As an example, the fragmentation pattern of oxidation product m/z 362, dGMP + O is presented in Figure 4. The most intense fragment ion (m/z 166) correlates to the modified nucleobase, guanosine + O. In addition, the fragment ion of the unmodified 2'-deoxyribose 5'-phosphate group is detected (m/z 195). Both fragments clearly prove that the oxidation has taken place in the nucleobase and not in the sugar phosphate moiety. The loss of NHCO, which appears for the precursor ion (m/z 319) as well as for the fragment of the nucleobase (m/z 123), is supposed to occur in the six membered ring, but can also result from a fragmentation in

the oxidized five membered ring. A subsequent loss of CO takes place, which is in agreement with an oxidation at position 8 of dGMP. Furthermore, the loss of water and ammonia from the nucleobase fragment ion is observed. To conclude, the determined molecular formula of the product and the fragmentation pattern are consistent with the formation of 2'-deoxy-8-oxoguanosine 5'-monophosphate (8-oxo-dGMP). 8-oxo-dGMP is one of the major oxidative DNA lesions [1–3] and a frequently studied biomarker for oxidative damage in vivo [34–36]. It has also been reported as an electrochemical generated oxidation product of dGMP in several studies based on CV measurements [11, 12, 37].

As discussed in detail for 8-oxo-dGMP, the fragmentation pattern of further oxidation products of dGMP was analyzed. For all oxidation products (Fig. 2) the presence of the fragment ion of the unmodified 2'-deoxyribose 5'-phosphate group proves that the nucleobase is the site of oxidation. Further fragment ions are in agreement with the suggested structures shown in Figure 5. However, based on the fragmentation, no definite structures can be determined, since as an example the loss of NHCO, which is observed as an intense fragment ion for a number of oxidation products, may result from different precursor structures. The dehydrogenation products m/z 345 and m/z 344 are known electrochemical oxidation products of dGMP, which undergo further reaction to 8-oxo-dGMP (m/z 362) [38, 39]. 8-oxo-dGMP is more readily oxidized than dGMP itself, due to its lower oxidation potential [40, 41] and is thus not the final oxidation product of dGMP. Further oxidation products are doubly (m/z 378, 380) and triply hydroxylated species (m/z 396). These oxidation products have been predicted by Goyal et al. [11] by studying cyclic voltammograms. The most intense oxidation product of dGMP appearing in the mass voltammogram, m/z 352, correlates to the formation of the nucleotide of guanidinohydantoin. The oxidation product m/z 335 may derive from the guanidinohydantoin nucleotide by a deamination reaction. The formation of the imidazolone structure of m/z 307 under oxidative conditions has been previously reported in the literature [42–44]. In addition to the oxidation products shown in the section of the mass voltammogram in Figure 2, oxidation products correlating to the molecular formulas $C_5H_8O_7P_1$ and $C_5H_{10}O_7P_1$ are generated at a potential of 2000 mV. The molecular formulas correspond to oxidized 2'-deoxyribose 5'-phosphate groups. Thus, an oxidative lesion of the nucleobase from the ribose phosphate group does take place at high potentials.

The oxidation products given in Figure 5 have been generated using a BDD working electrode at an oxidation potential up to 2500 mV. Taking these conditions into account, it is very likely that the formation of hydroxyl radicals in the electrochemical cell does take place [31–33]. Thus, the oxidation products may result from direct electron abstraction, but also from adduct formation with hydroxyl radicals as well as via hydrogen abstraction by hydroxyl radicals.

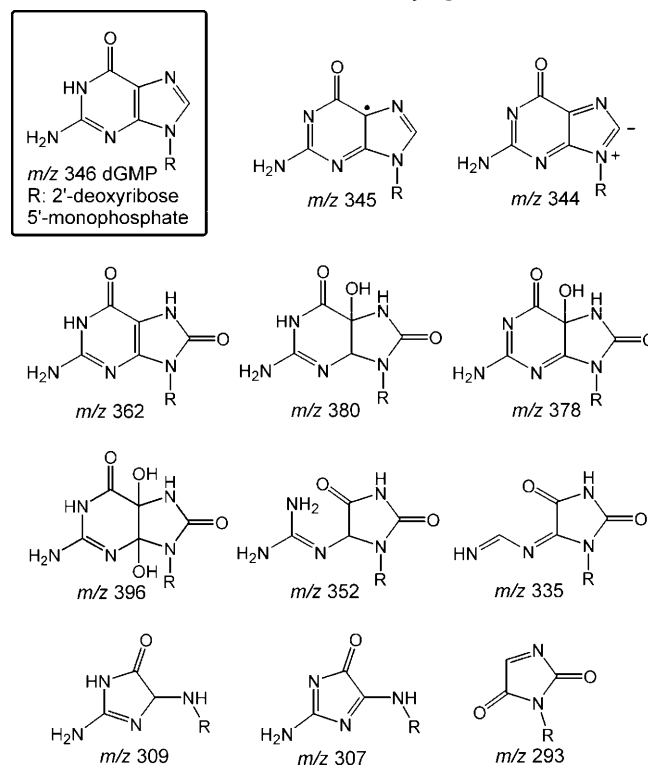


Fig. 5. Postulated structures of dGMP and dGMP oxidation products. Structures are in accordance with product ion spectra obtained by on-line EC/ESI-MS/MS and the exact masses determined by EC/ESI-ToF/MS.

A section of the mass voltammogram of dCMP, obtained by on-line EC/ESI-ToF/MS measurements is shown in Figure 6. A significant signal increase is observed in the potential range above 1800 mV. As described for dGMP, an oxidative lesion of the 2'-deoxyribose 5'-phosphate group can be observed. Further oxidation products are one, two and three times hydroxylated dCMP species. In the organism, oxidative DNA damage may result in the formation of 5-hydroxycytosine and cytosine glycol. Cytosine glycol is known to be relatively instable and undergoes subsequent reactions, resulting in the formation of 5-hydroxyuracil and uracil glycol [45, 46–48]. As indicated by the structures in Figure 6, observed oxidation products + O and + O + 2H in the mass voltammogram correlated to the formation of 2'-deoxy-5-hydroxycytidine 5'-phosphate and 2'-deoxycytidine glycol 5'-phosphate upon oxidation at the BDD working electrode.

Furthermore, the mass voltammograms of dAMP, dUMP and the RNA base dTMP were acquired (mass voltammograms not shown). In case of dAMP, oxidation was observed at a potential above 2000 V. As described for dGMP, a signal of the oxidized 2'-deoxyribose 5'-phosphate group appears at high potential. Besides that, minor oxidation products are observed, but can not be identified. The formation of hydroxylation products like 2,8-dihydroxyadenosine as well as dimeric products, which have been previously reported in the literature [10, 49] was not observed. The nucleotides dUMP and dTMP show the formation of + O, + 2O, + 2O +

These are not the final page numbers!

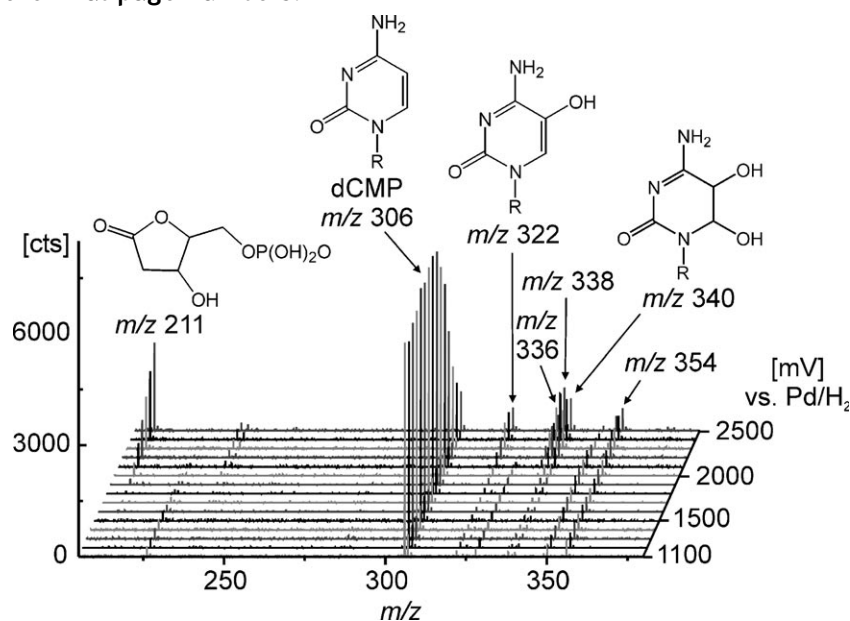


Fig. 6. Section of the mass voltammogram of dCMP. Tentative structures of oxidation products are given above the peaks.

2H products. This correlates to the formation of glycol structures, which are also known to appear as an oxidative lesion *in vivo* [50–52]. In case of dTMP, an additional oxidation of the methyl group is assumed due to a +O-2H product appearing in the mass voltammogram.

4. Conclusions

Based on the hyphenation of electrochemistry and mass spectrometry, the electrochemical oxidation behavior of nucleotides was studied. The on-line set-up allows the generation and direct identification of the oxidation products by ESI-ToF/MS and ESI-MS/MS, without previous isolation or derivatization steps. Compared with classical cyclovoltammetric methods, the presented approach rapidly provides important information on the nature and possibly on the concentration of the formed oxidation products. Even transient species like dehydrogenated dGMP and 2'-deoxycytidine glycol 5'-phosphate can be detected. Coupling EC/ESI-MS to liquid chromatography might provide additional information on the polarity of the oxidation products. Oxidation was performed in an electrochemical thin-layer cell, equipped with a boron doped diamond electrode. Due to its specific characteristics like the anodic generation of hydroxyl radicals and the inert surface, BDD is especially well suited to generate nucleotide oxidation products which also occur upon DNA damage by ROS *in vivo*. BDD is in general known to show a high overpotential to processes requiring the adsorption of reaction intermediates on the surface [31]. Thus, previously reported dimeric or tetrameric oxidation products were not observed in the present study [12]. For dGMP and dCMP, good conversion rates were achieved, allowing advanced structure elucidation of dGMP oxidation products by ESI-MS/MS. Further

developments in the electrochemical technique, for example the combination of the direct electrochemical oxidation with Fenton reactions [14], have the potential to further increase the oxidative conversion of nucleotides. The comparison of the presents results with oxidative DNA damage occurring in the organism shows that the formation of mutagenic DNA lesions like 8-oxo-dGMP, 2'-deoxy-5-hydroxycytidine 5'-monophosphate, 2'-deoxycytidine glycol 5'-monophosphate as well as hydroxylated dUMP and dTMP species was successfully achieved in the EC-MS set-up.

5. References

- [1] M. J. Marnett, *Carcinogenesis* **2000**, *21*, 361.
- [2] D. Wang, D. A. Kreuzer, J. M. Essigmann, *Mutat. Res.* **1998**, *400*, 99.
- [3] H. Kamiya, *Nucleic Acid Res.* **2003**, *31*, 517.
- [4] M. Valko, C. J. Rhodes, J. Moncol, M. Izakovic, M. Mazur, *Chem.-Biol. Interact.* **2006**, *160*, 1.
- [5] C. J. Burrows, J. G. Muller, *Chem. Rev.* **1998**, *98*, 1109.
- [6] S. Shibutani, M. Takeshita, A. P. Grollmann, *Nature* **1991**, *349*, 431.
- [7] C. Tagesson, M. Kallberg, C. Klintonberg, H. Starkhammar, *Eur. J. Cancer* **1995**, *31A*, 934.
- [8] C. Lengger, G. Schoch, H. Topp, *Anal. Biochem.* **2000**, *287*, 65.
- [9] A. M. Oliveira-Brett, J. A. P. Piedade, L. A. Silva, V. C. Diculescu, *Bioanal. Chem.* **2004**, *332*, 321.
- [10] R. N. Goyal, A. Sangal, *J. Electroanal. Chem.* **2002**, *521*, 72.
- [11] R. N. Goyal, S. M. Sondhi, A. M. Lahoti, *New J. Chem.* **2005**, *29*, 587.
- [12] F. Boussicault, M. Robert, *Chem. Rev.* **2008**, *180*, 2622.
- [13] E. E. Ferapontova, E. Dominguez, *Electroanalysis* **2003**, *15*, 629.
- [14] J. J. Zhang, B. Wang, Y. F. Li, W. L. Jia, H. Cui, H. S. Wang, *Electroanalysis* **2008**, *20*, 1684.

- [15] T. G. Drummond, M. G. Hill, J. K. Barton, *Nat. Biotechnol.* **2003**, *21*, 1192.
- [16] D. Porath, A. Bezryadin, S. de Vries, C. Dekker, *Nature* **2000**, *403*, 635.
- [17] K. A. Friedman, A. Heller, *J. Phys. Chem. B* **2001**, *105*, 11859.
- [18] G. Hambitzer, J. Heitbaum, *Anal. Chem.* **1986**, *58*, 1067.
- [19] K. J. Volk, M. S. Lee, R. A. Yost, A. Brajter-Toth, *Anal. Chem.* **1988**, *60*, 720.
- [20] K. J. Volk, R. A. Yost, A. Brajter-Toth, *Anal. Chem.* **1989**, *61*, 1709.
- [21] W. Lohmann, U. Karst, *Anal. Bioanal. Chem.* **2009**, *394*, 1341.
- [22] W. Lohmann, U. Karst, *Anal. Bioanal. Chem.* **2008**, *391*, 79.
- [23] T. A. Getek, W. A. Korfmacher, T. A. McRae, J. A. Hinson, *J. Chromatogr. A* **1989**, *474*, 245.
- [24] H. Deng, G. J. VanBerkel, *Electroanalysis* **1999**, *11*, 857.
- [25] P. H. Gamache, D. F. Meyer, M. C. Granger, I. N. Acworth, *J. Am. Soc. Mass Spectrom.* **2004**, *15*, 1717.
- [26] S. M. Van Leeuwen, B. Blankert, J.-M. Kauffmann, U. Karst, *Anal. Bioanal. Chem.* **2005**, 382, 742.
- [27] W. Lohmann, U. Karst, *Anal. Chem.* **2007**, *79*, 6831.
- [28] U. Jurva, H. V. Wikström, A. P. Bruins, *Rapid Commun. Mass Spectrom.* **2000**, *14*, 529.
- [29] A. Baumann, B. Schubert, H. Oberacher, U. Karst, *J. Chromatogr. A* **2009**, *1216*, 3192.
- [30] N. A. Mautjana, J. Estes, J. R. Eyler, A. Brajter-Toth, *Electroanalysis* **2008**, *20*, 2501.
- [31] A. Kraft, *Int. J. Electrochem. Sci.* **2007**, *2*, 355.
- [32] H. B. Martin, A. Argoitia, U. Landau, A. B. Anderson, J. C. Angus, *J. Electrochem. Soc.* **1994**, *143*, L133.
- [33] B. Marselli, J. Garcia-Gomez, P.-A. Michaud, M. A. Rodrigo, C. Comninellis, *J. Electrochem. Soc.* **2003**, *150*, D79.
- [34] M. K. Shigenaga, C. J. Gimeno, B. N. Ames, *Proc. Natl. Acad. Sci.* **1989**, *86*, 9697.
- [35] F. Teichert, P. Greaves, J. F. Thorpe, R. D. Verschoyle, J. Kilian Mellon, W. P. Steward, P. B. Farmer, A. J. Gescher, R. Singh, *Rapid Commun. Mass Spectrom.* **2009**, *23*, 258.
- [36] D. Managal, D. Vudathala, J. H. Park, S. H. Lee, T. M. Penning, I. A. Blair, *Chem. Res. Toxicol.* **2009**, *22*, 788.
- [37] A. M. Oliveira Brett, J. A. P. Piedade, S. H. P. Serrano, *Electroanalysis* **2000**, *12*, 969.
- [38] J. Cadet, M. Berger, G. W. Buchko, P. C. Joshi, S. Raoul, J.-L. Ravanat, *J. Am. Chem. Soc.* **1994**, *116*, 7403.
- [39] L. P. Candeias, S. Steenken, *J. Phys. Chem.* **1992**, *96*, 937.
- [40] S. Steenken, S. V. Jovanovic, *J. Am. Chem. Soc.* **1997**, *119*, 617.
- [41] T. Z. Markus, S. S. Daube, R. Naaman, A. M. Fleming, J. G. Muller, C. J. Burrows, *J. Am. Chem. Soc.* **2009**, *131*, 89.
- [42] G. Pratviel, B. Meunier, *Chem.-Eur. J.* **2006**, *12*, 6018.
- [43] V. Duarte, D. Gasparutto, L. F. Yamaguchi, J.-L. Ravanat, G. R. Martinez, M. H. G. Medeiros, P. Di Mascio, J. Cadet, *J. Am. Chem. Soc.* **2000**, *122*, 12622.
- [44] W. Luo, J. G. Muller, E. M. Rachlin, C. J. Burrows, *Chem. Res. Toxicol.* **2001**, *14*, 927.
- [45] R. Olinski, T. Zastawny, J. Budzbon, H. Kasai, *FEBS Lett.* **1992**, *309*, 193.
- [46] M. Dizdaroglu, E. Holwitt, M. P. Hagan, W. F. Blakely, *Biochem. J.* **1986**, *235*, 531.
- [47] S. Tremblay, J. R. Wagner, *Nucleic Acid Res.* **2008**, *36*, 284.
- [48] T. Douki, T. Delatour, F. Paganon, J. Cadet, *Chem. Res. Toxicol.* **1996**, *9*, 1145.
- [49] R. N. Goyal, A. Sangal, *J. Electroanal. Chem.* **2003**, *557*, 147.
- [50] M. E. Hegi, T. P. Sageldorff, W. K. Lutz, *Carcinogenesis* **1989**, *10*, 43.
- [51] M. Weinfeld, J. Z. Xing, J. Lee, S. A. Leadon, P. K. Cooper, X. C. Le, *Prog. Nucleic Acid Res. Mol. Biol.* **2001**, *68*, 139.
- [52] X. C. Le, J. Z. Xing, J. Lee, S. A. Leadon, M. Weinfeld, *Science* **1998**, *280*, 1066.